Supplementary Table

Sequences

siRNA target	Sense Strand (5'→3')
Bglap1	AAACGCAUCUAUGGUAUCAUU
Cdh16	GGUAGAGCCUGGUGAAUACUU
Gfp	GGCUACGUCCAGGAGCGCACC
Il12a	GAAUCAUAAUGGCGAGACUUU
Irf3	AAACCUACCGAAGUUAUUUUU
Luc (23-nt)	CAUAAGGCUAUGAAGAGAUACdTdT
Luc (21-nt)	UAAGGCUAUGAAGAGAUACdTdT
Luc (19-nt)	UAAGGCUAUGAAGAGAUdTdT
Luc (16-nt)	UAAGGCUAUGAAGAdTdT
Luc (13-nt)	UAAGGCUAUGAdTdT
Luc (7-nt)	UAAGGdTdT
RISC-free	Proprietary
RS1	UAGCGACUAAACACAUCAAUU
RS2	GCGCGCUUUGUAGGAUUCGdTdT
RS3	AGUACAGCAAACGAUACGGdTdT
RS4	AGUACUGCAUACGAUACGGTT
RS5	AGUACUACUUACGAUACGGTT
RS6	CGUACUGCUUGCGAUACGGTT
Sftpb	ACAAGAAUGUGAUAUCCUUUU
Tlr3	GGAUGUUUUCGGGCCGCCUdTdT
hVegfa	ACCUCACCAAGGCCAGCACdTdT
mVegfa (for laser injury)	ACCUCACCAAAGCCAGCACdTdT
mVegfa (for dermal wounding)	CGAUGAAGCCCUGGAGUGCdTdT
Vegfr1	CUGAGUUUAAAAGGCACCCdTdT

Chemical modifications

siRNA-*Luc* (21-nt)	Sense strand	Anti-sense strand
Cholesterol	3’ conjugation	Unmodified
Fluorescein	5’ conjugation	Unmodified
CH_3O	Unmodified	5’ substitution
2’O-methyl	Alternating substitutions, starting with first nucleoside	Alternating substitutions, starting with second nucleoside

Supplementary Figure S1

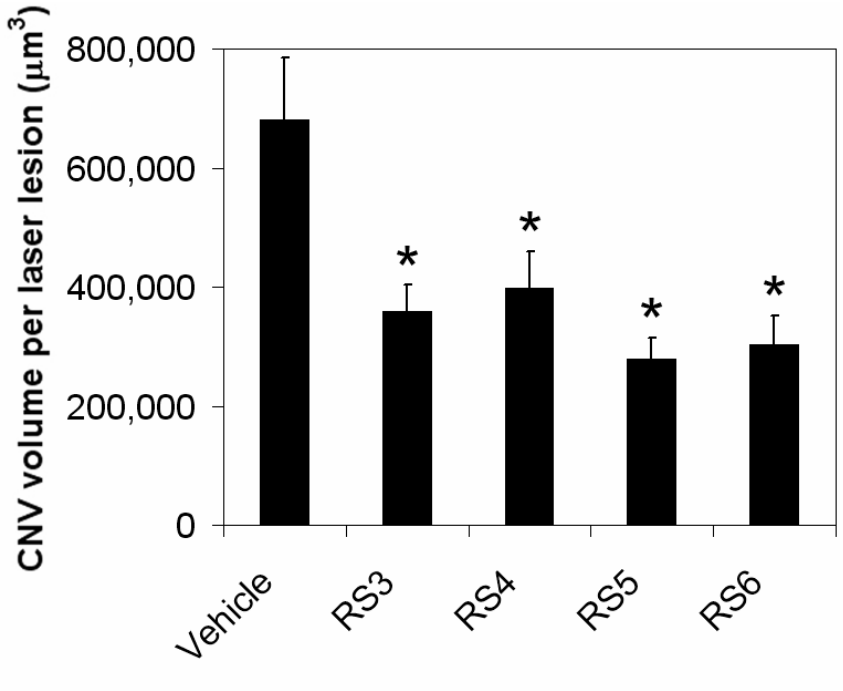

Random sequence siRNAs suppressed CNV. Intravitreous administration of 1 µg of any of four siRNAs comprising random sequences (RS3-6; Supplementary Table) without sequence identity to known genomic sequences uniformly suppressed CNV in wild-type mice. n=8, * $P < 0.05$ compared to vehicle (siRNA buffer).

Supplementary Figure S2

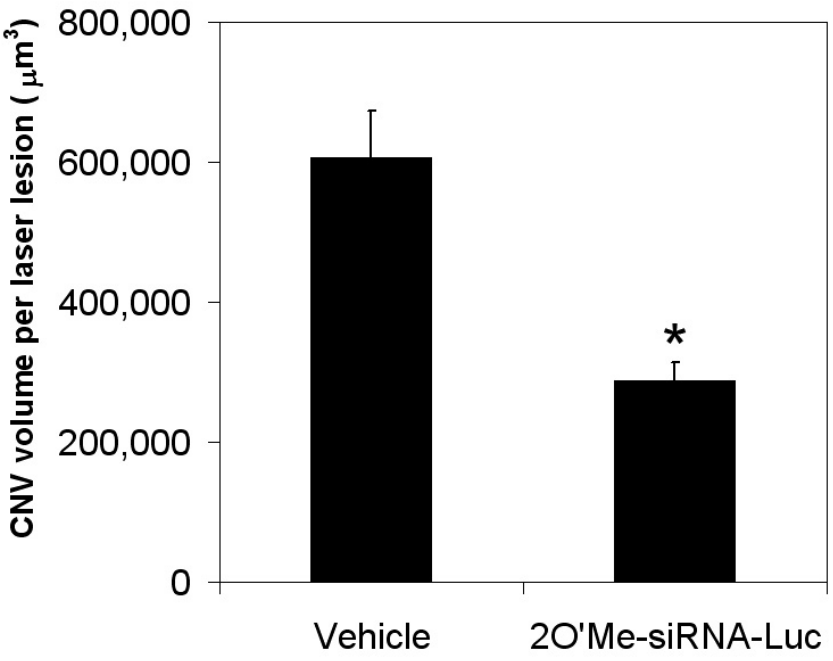

Systemic non-targeted siRNA suppressed CNV. Intraperitoneal administration of serum-stable 2'*O*-methyl-siRNA-*Luc* (6 mg/kg) suppressed CNV in wild-type mice. n=6, * $P < 0.05$ compared to vehicle (PBS).

Supplementary Figure S3

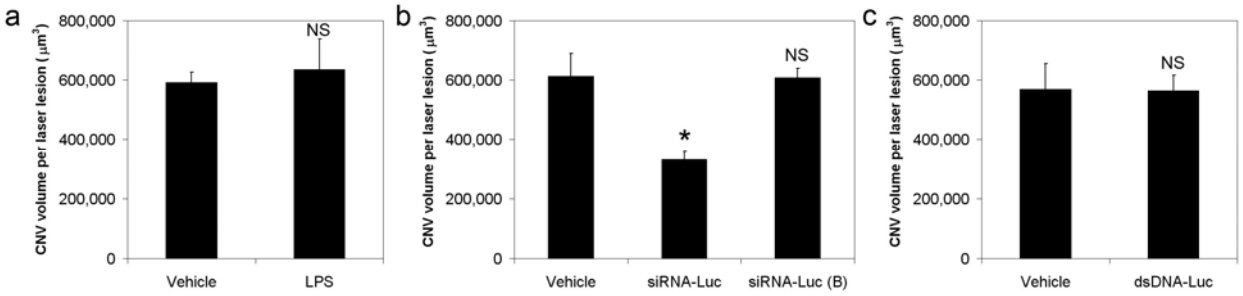

Specificity of CNV suppression by non-targeted siRNA. a, Intravitreous administration of *E. coli K12* lipopolysaccharide (LPS; 1 μg) did not suppress CNV in wild-type mice compared to vehicle (PBS); n=5. **b,** Digestion of siRNA-*Luc* (1 μg) with Benzonase® (B) abrogated the former's ability to suppress CNV in wild-type mice. n=5, * $P < 0.05$. **c,** A double stranded DNA analogue of siRNA-*Luc* (dsDNA-*Luc*; 1 μg) did not suppress CNV in wild-type mice compared to vehicle (PBS). n=5. NS, No significant difference compared to vehicle.

Supplementary Figure S4

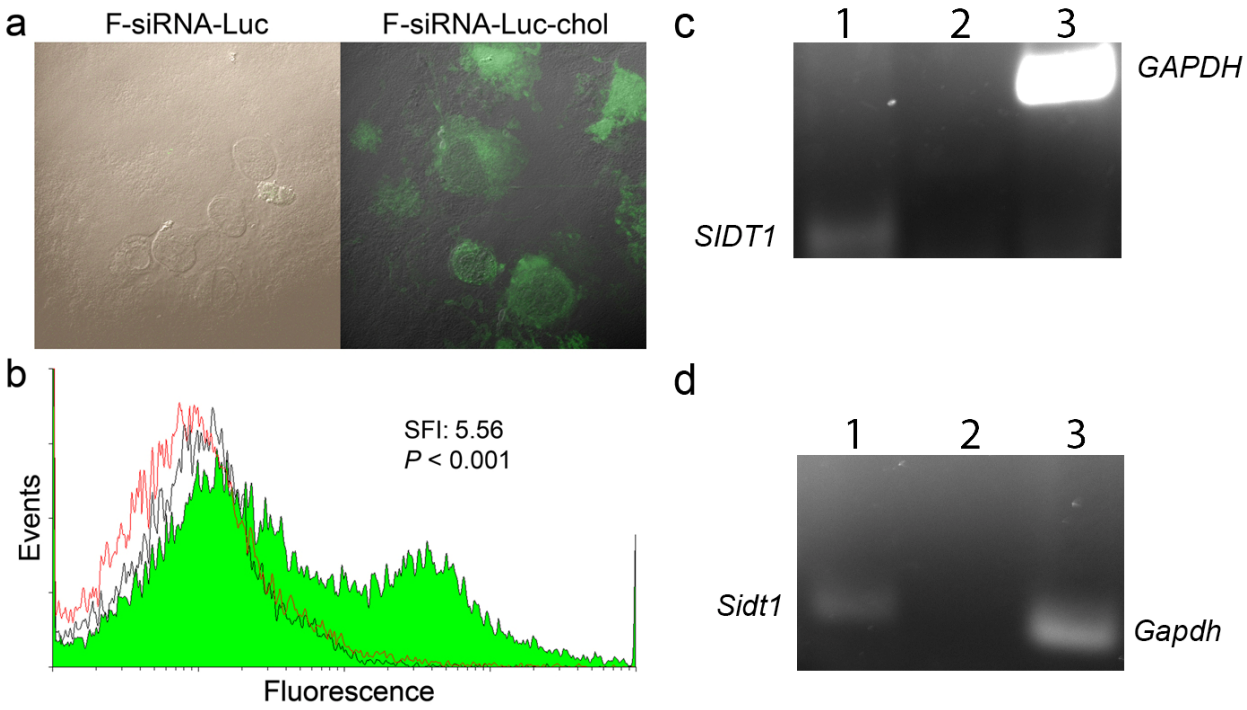

Internalization of siRNA. a, Fluorescein (F)-conjugated siRNA-*Luc* was internalized by primary human choroidal endothelial cells as shown by immunofluorescence (green channel overlaid on Nomarski images) if it was conjugated to cholesterol (right panel) but was not internalized in naked form (left panel) and (**b**) by mouse RPE/choroidal cells in cholesterol-conjugated form (green curve) but not in naked form (red curve), as shown by flow cytometry. Black curve corresponds to cells not exposed to siRNA. Human or mouse cells were incubated with siRNAs for 1 h. n=3. SFI, standardized fluorescence index (ratio of geometric means of cells exposed to F-siRNA-*Luc*-chol (shaded) to cells exposed to F-siRNA-*Luc* (red curve), *P* values reflect statistical comparison between curves. **c,d,** *Sidt1* mRNA expression in human CECs (**c**) and mouse RPE/Choroid (**d**) was analyzed by RT-PCR and gel electrophoresis (n=3). Gel lanes are (**c**) 1: *SIDT1* with cDNA; 2: *SIDT1* without cDNA (H_2O); 3: *GAPDH* and (**d**) 1: *Sidt1* with cDNA; 2: *Sidt1* without cDNA (H_2O); 3: *Gapdh*. The observed bands matched the predicted amplicon sizes (*SIDT1*: 130bp; *GAPDH*: 299bp; *Sidt1*: 138 bp; *Gapdh*: 121 bp).

Supplementary Figure S5

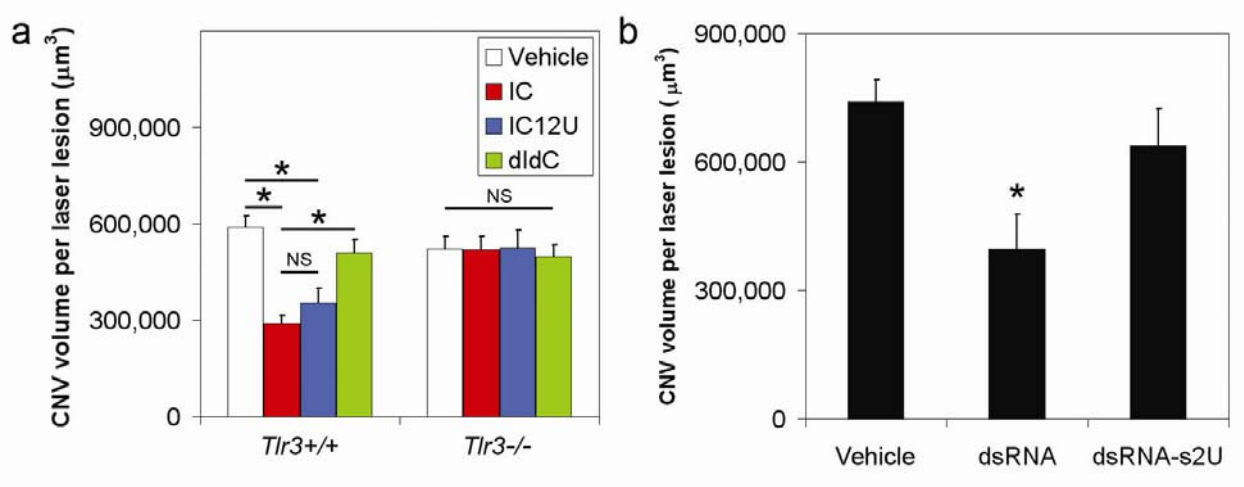

Long double stranded RNAs suppress CNV via TLR3. a, Intravitreous administration of 2 μg of polyinosinic:polycytidylic acid (IC) and poly I:C_{12}U (Ampligen®, wherein uridine replaces cytosine statistically at every 13th nucleoside; IC12U), but not polydeoxyinosinic:polydeoxycytidylic acid (dIdC; 2 μg), suppressed CNV in *Tlr3*$^{+/+}$ mice but not in *Tlr3*$^{-/-}$ mice. Vehicle (PBS); n=5-9, * $P < 0.05$; NS, not significant. **b,** Intravitreous administration of 2 μg of *in vitro* transcribed dsRNA (~1,000 nt), but not 2-thiouridine (s2U) modified dsRNA that does not activate TLR3, suppressed CNV in wild-type mice. n=5, * $P <$ 0.05 compared to vehicle (PBS).

Supplementary Figure S6

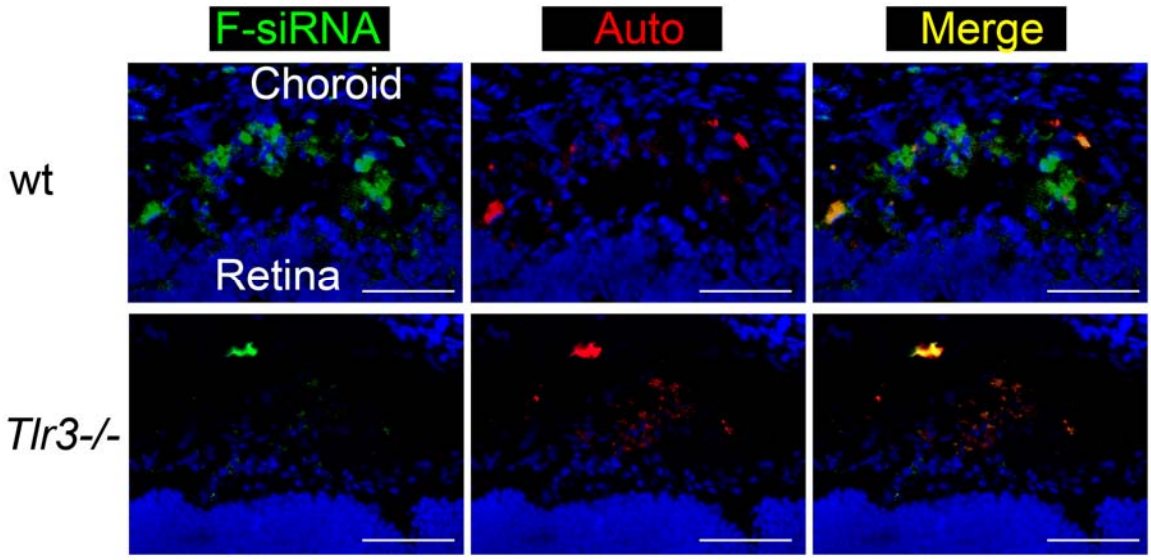

***In situ* binding of siRNA to TLR3-expressing eye sections.** Fluorescein-conjugated siRNA-*Luc* (F-siRNA) bound to unfixed frozen sections of wild-type (wt) but not *Tlr3*$^{-/-}$ mouse eyes in the area of laser injury. Autofluorescence is shown in red. Green/red merged images are shown to demonstrate specific binding.

Supplementary Figure S7

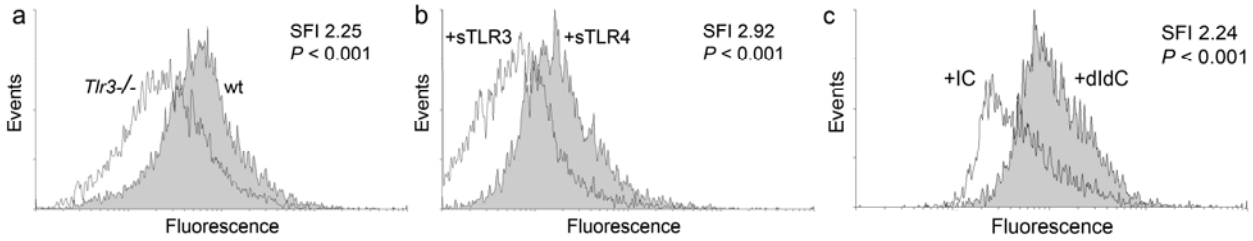

Detection of F-siRNA binding to TLR3. a, Flow cytometry detected greater emitted fluorescence from $CD31^{+}VEGFR2^{+}$ endothelial cells isolated from wild-type mouse choroid 1 day after laser injury than *Tlr3*$^{-/-}$ choroidal endothelial cells (CECs) when incubated with fluorescein-conjugated siRNA-*Luc* (F-siRNA). **b,** Pre-incubation of F-siRNA with recombinant soluble (s) TLR3 suppressed fluorescence emitted from wild-type mouse CECs to a greater extent than pre-incubation with sTLR4. **c,** Pre-treatment of cells with the TLR3 ligand poly I:C suppressed fluorescence emitted from wild-type mouse CECs incubated with F-siRNA to a greater extent than pre-incubation with poly dI:dC. n=3, SFI, standardized fluorescence index (ratio of geometric means of cell populations), *P* values reflect statistical comparison between curves.

Supplementary Figure S8

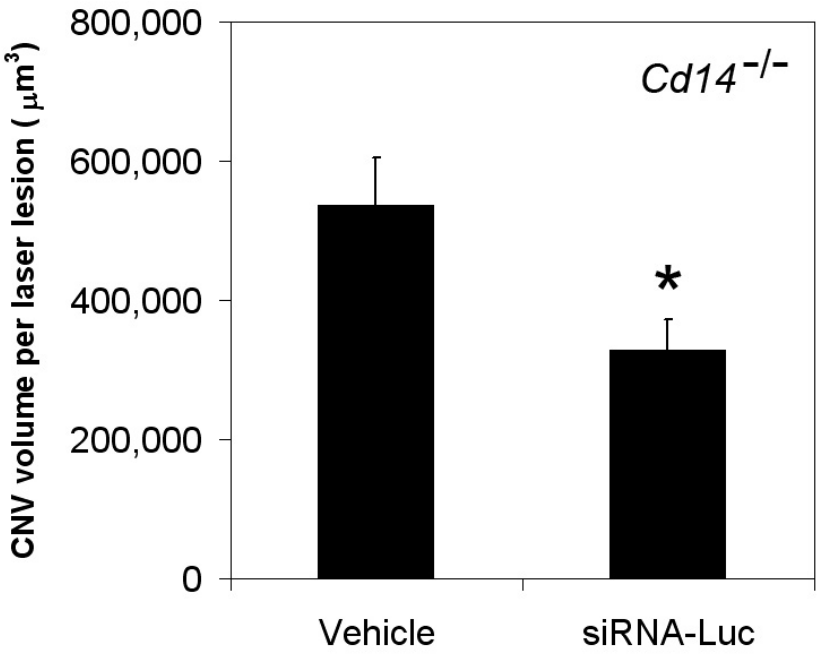

CD14 not required for siRNA suppression of CNV. Intravitreous administration of siRNA-*Luc* (1 μg) suppressed CNV in *Cd14*$^{-/-}$ mice. n=6, * $P < 0.05$ compared to vehicle (siRNA buffer).

Supplementary Figure S9

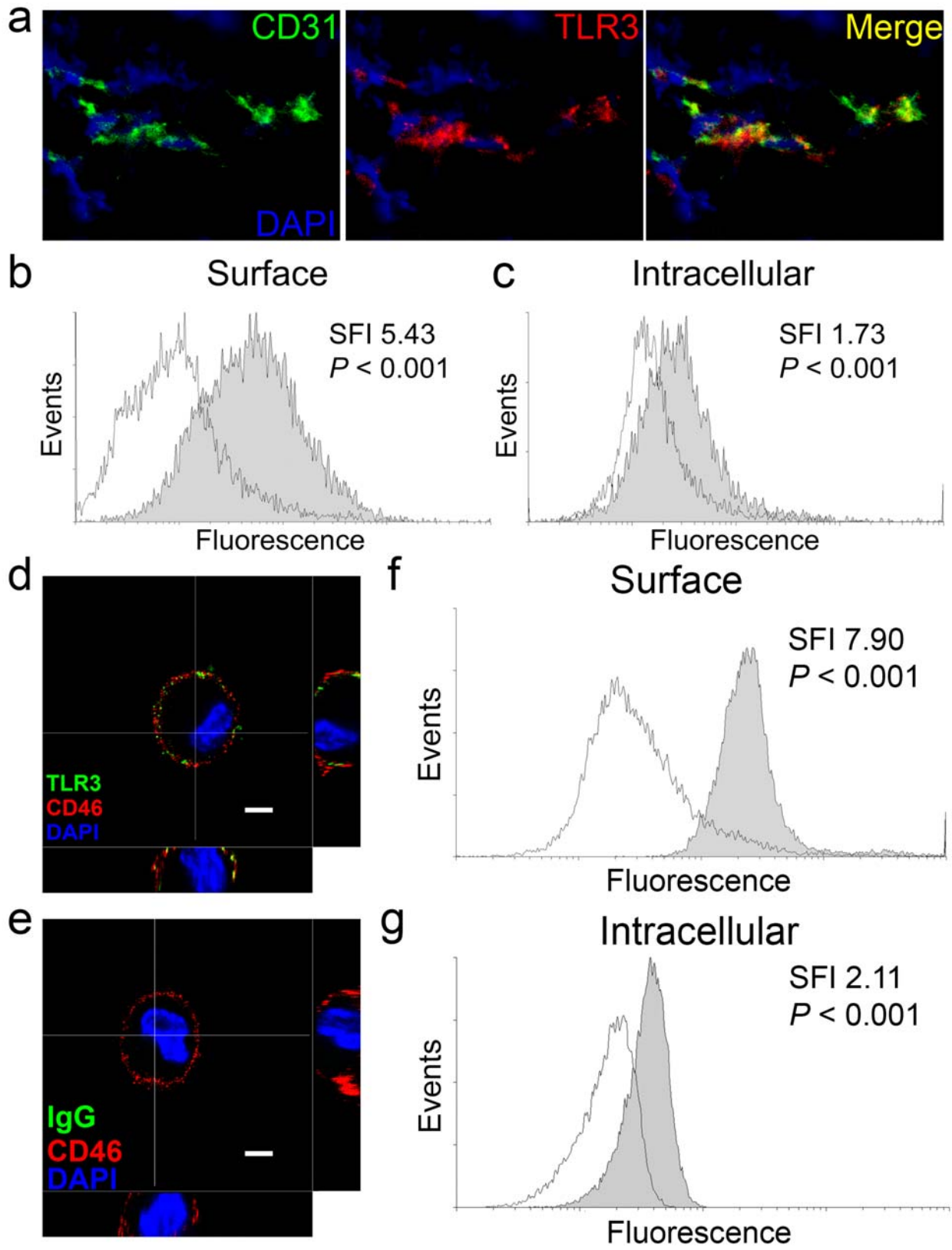

Choroidal endothelial cells express TLR3. a, Immunofluorescence showed multiple areas of superimposition of TLR3 (red) and cell surface marker CD31 (green) signals in the choroid of wild-type mice at the site of laser injury. Images representative of 3 experiments. Nuclei stained with DAPI. **b,c,** Flow cytometry on wild-type mouse choroidal endothelial cells (CECs; defined as $CD31^{+}VEGFR2^{+}$ cells isolated from RPE/choroid) 1 day after laser injury without (**b**) and with (**c**) permeabilization showed that TLR3 was expressed predominantly on their surface. **d,e,** Orthogonal views obtained by laser scanning confocal microscopy showed (**d**) co-localization of the cell surface glycoprotein CD46 (red) and TLR3 (green) with DAPI counterstain in non-permeabilized human CECs. No staining was observed with isotype IgG in place of anti-TLR3 Ab (**e**). Scale bars, 5 μm. **f,g,** Flow cytometry without (**f**) and with (**g**) permeabilization showed that TLR3 was expressed predominantly on surface of primary human CECs. (**b,c,f,g**) Shaded region, TLR3 Ab; Unshaded region, Isotype IgG. SFI, standardized fluorescence index (ratio of geometric mean of TLR3 stained versus isotype stained populations). *P* values compare TLR3 versus isotype stained curves.

Supplementary Figure S10

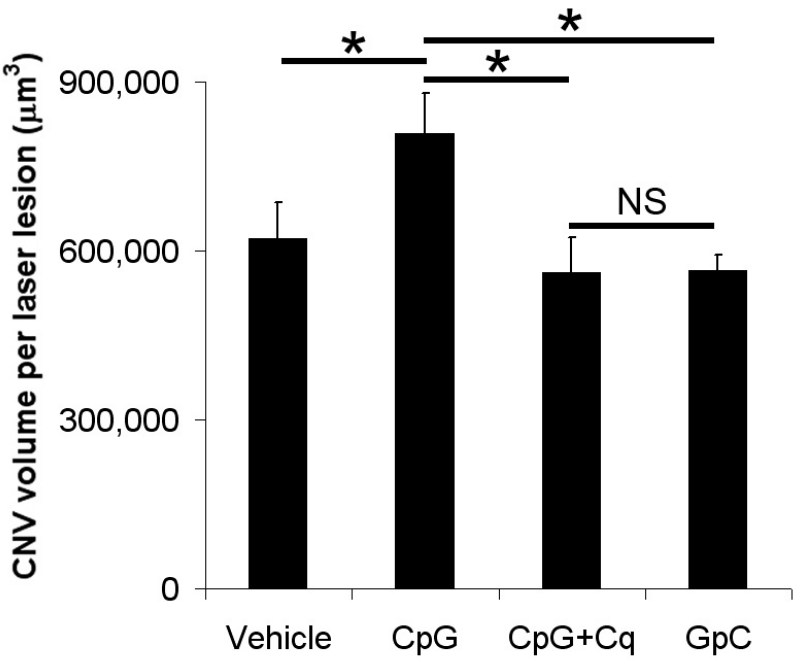

TLR9 stimulation-induced CNV increase was sensitive to chloroquine. Intravitreous injection of 2 μg of immunostimulatory CpG oligonucleotide (ODN) increased CNV compared to vehicle (PBS) or GpC ODN. Chloroquine (Cq; 30 ng) co-administration abolished CpG ODN-induced increase in CNV. n=6-9, * $P < 0.05$, NS, not significant.

Supplementary Figure S11

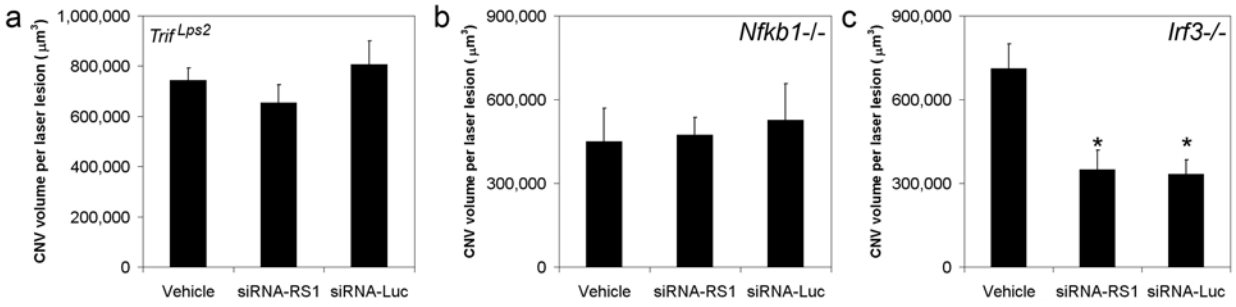

CNV suppression by non-targeted siRNA diverges at the level of TRIF. Intravitreous administration of siRNA-RS1 and siRNA-*Luc* (1 μg each) did not suppress CNV in *Trif*^{Lps2} (**a**) or *Nfkb1*$^{-/-}$ mice (**b**) but did suppress CNV in *Irf3*$^{-/-}$ mice (**c**). n=6, * $P < 0.05$ compared to vehicle (siRNA buffer).

Supplementary Figure S12

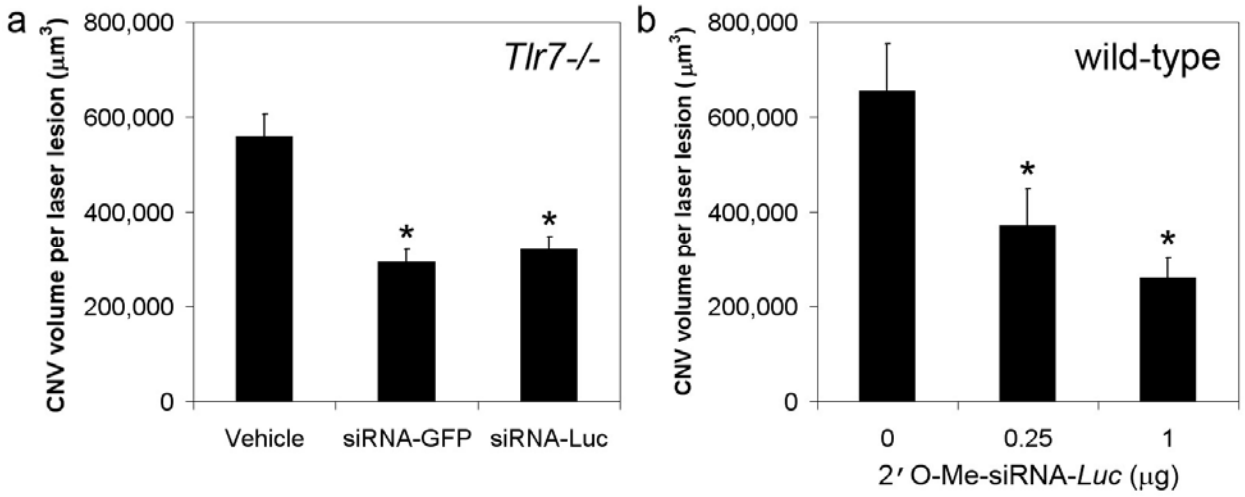

TLR7 not required for CNV suppression. Intravitreous administration of siRNA-GFP or siRNA-*Luc* (1 μg each) suppressed CNV in *Tlr7*$^{-/-}$ mice. (**b**) 2'*O*-methyl-siRNA-*Luc* suppressed CNV in wild-type mice in a dose-dependent fashion. n=6, * $P < 0.05$ compared to vehicle (siRNA buffer).

Supplementary Figure S13

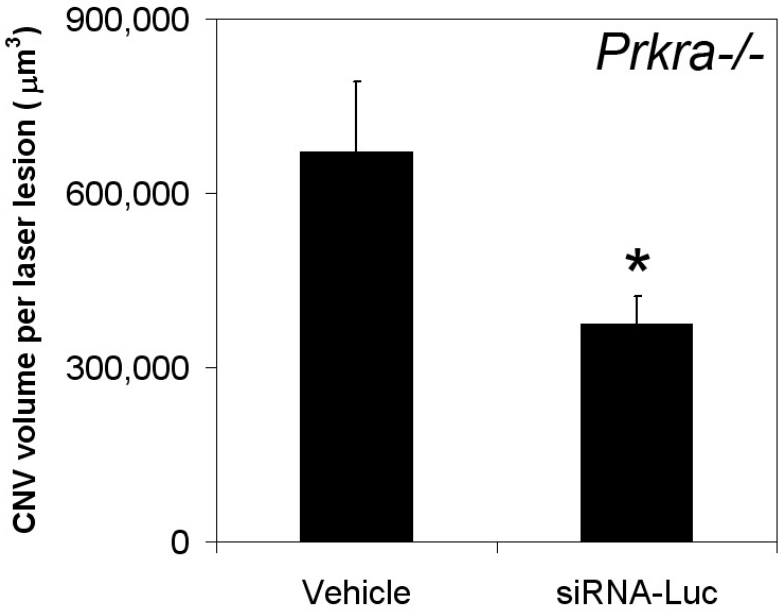

PKR not required for siRNA-induced CNV suppression. Intravitreous administration of siRNA-*Luc* (1 μg) suppressed CNV in *Prkra*$^{-/-}$ mice. n=6, * $P < 0.05$ compared to vehicle (siRNA buffer).

Supplementary Figure S14

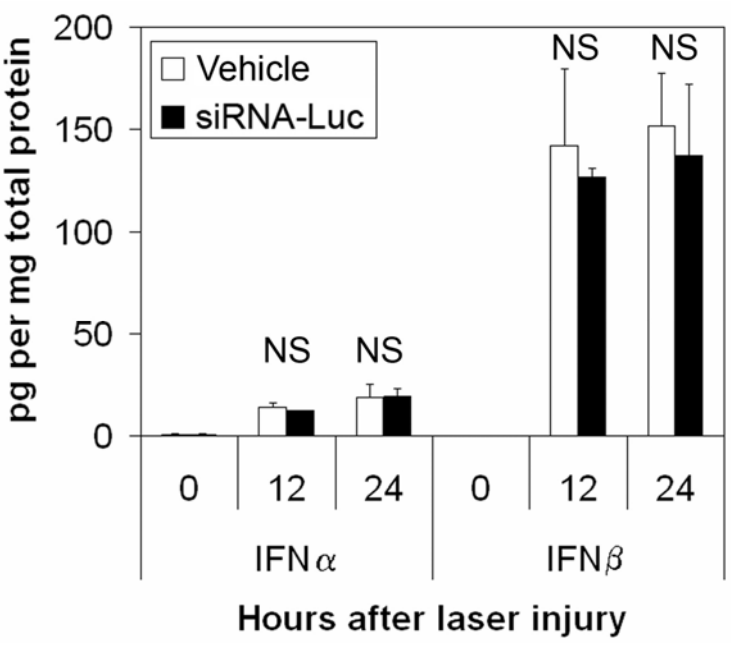

siRNA does not upregulate type I IFN. Levels of interferon (IFN)-α and IFN-β proteins in the retinal pigmented epithelium (RPE)/choroid at 12 or 24 h after laser injury were not significantly (NS) different between wild-type mouse eyes injected with siRNA-*Luc* (1 μg) and those injected with vehicle. n=12.

Supplementary Figure S15

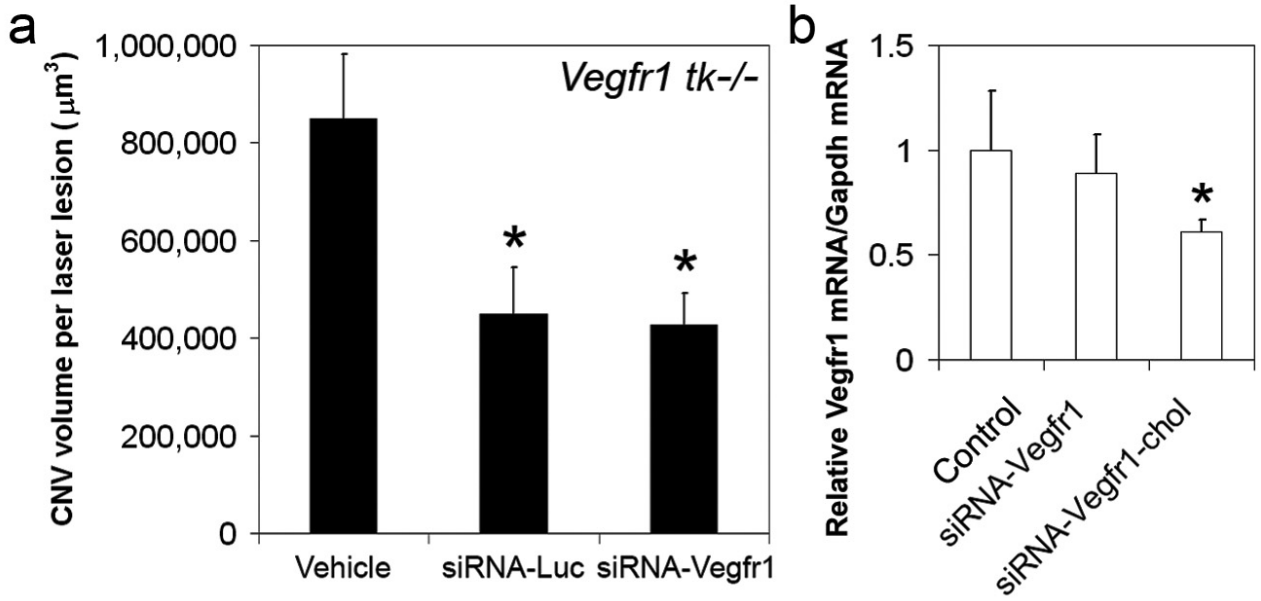

siRNA-*Vegfr1* suppressed CNV in the absence of mRNA knockdown or protein signalling. **a,** siRNA-*Vegfr1* suppressed CNV in *Vegfr1 tyrosine kinase (tk)*$^{-/-}$ mice as effectively as siRNA-*Luc*. n=8. **b,** *Vegfr1* mRNA expression in RPE/choroid of *Tlr3*$^{-/-}$ mice was reduced by siRNA-*Vegfr1*-chol, whose 3' end was conjugated with cholesterol (chol), which enables intracellular entry, but not by siRNA-*Vegfr1*. n=8-9. Gene expression 16 h after administration measured by real time RT-PCR was normalized to *Gapdh* mRNA levels and to baseline levels. siRNAs (1 μg) were injected intravitreously.

Supplementary Figure S16

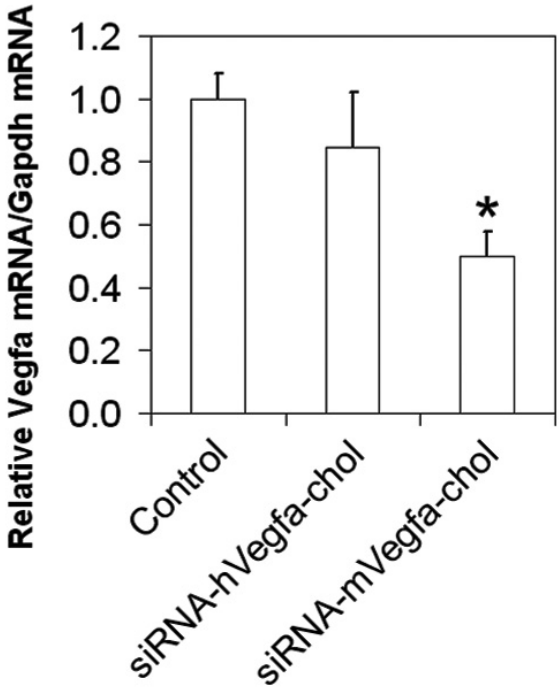

Intracellularly delivered siRNA-*Vegfa* required complete complementarity to knockdown mRNA. *Vegfa*164 mRNA expression in RPE/choroid of *Tlr3*$^{-/-}$ mice was reduced by siRNA-m*Vegfa*-chol but not by siRNA-h*Vegfa*-chol. n=6, * $P < 0.05$ compared to control (baseline uninjected). Gene expression 16 h after administration measured by real time RT-PCR was normalized to *Gapdh* mRNA levels and to baseline levels. siRNAs (1 µg) were injected intravitreously.

Supplementary Figure S17

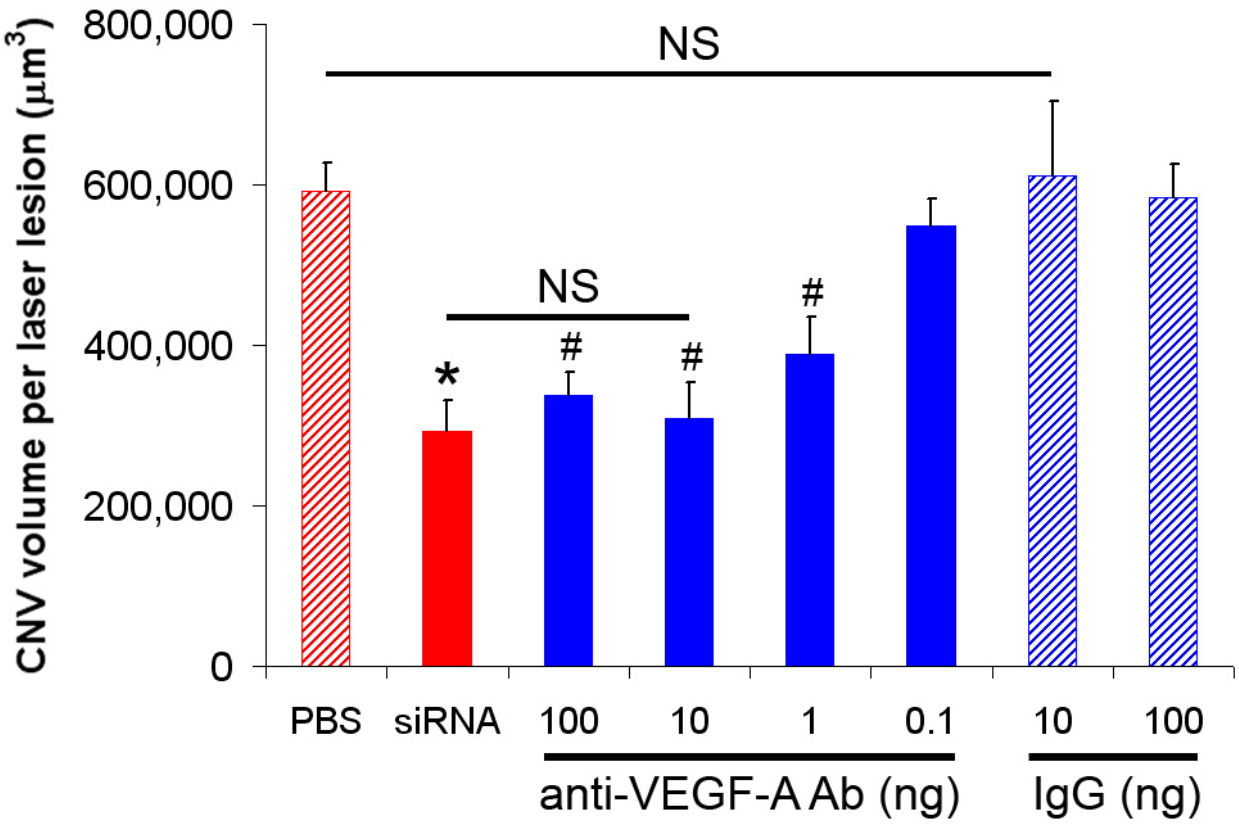

Non-targeted siRNA as effective as anti-VEGF-A Ab. Intravitreous administration of siRNA-*Luc* (1 µg) suppressed CNV in wild-type mice as effectively as neutralizing anti-VEGF-A antibodies (Ab). n=10-24, * $P < 0.05$ compared to PBS, # $P < 0.05$ compared to IgG, NS, not significant.

Supplementary Figure S18

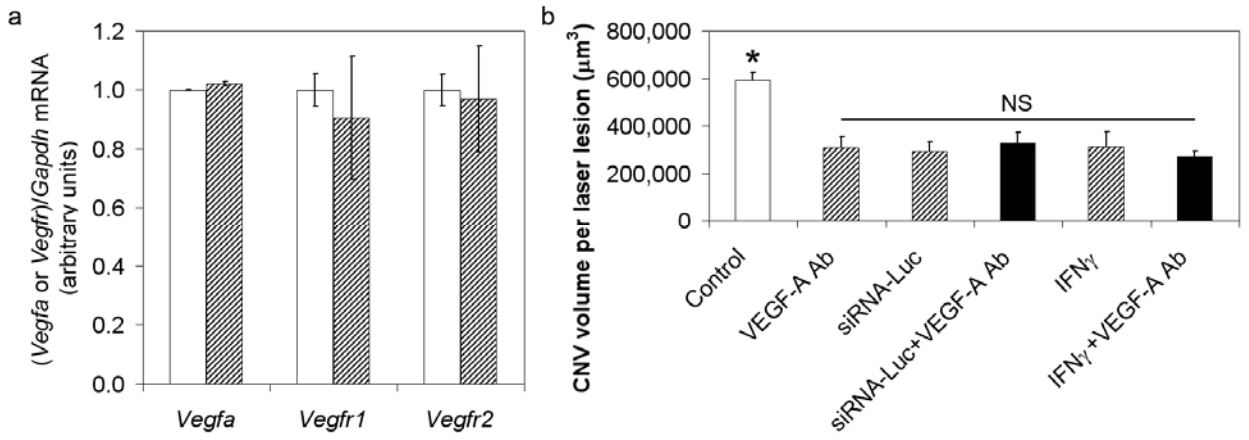

siRNA effect is independent of but not synergistic with VEGF-A pathway. a, Levels of *Vegfa*164, *Vegfr1*, and *Vegfr2* mRNAs in RPE/choroid of wild-type mice were not changed by siRNA-*Luc* (1 µg; shaded bars) compared with siRNA buffer (unshaded bars) 16 h after intravitreous administration. Gene expression measured by real time RT-PCR was normalized to *Gapdh* mRNA levels and to baseline levels. n=6, No significant differences between siRNA and buffer treated groups. **b,** Addition of neutralizing anti-VEGF-A antibodies (Ab; 10 ng; solid bars) did not enhance suppression of CNV in wild-type mice induced by intravitreous administration of siRNA-*Luc* (1 µg; shaded bar) or recombinant IFN-γ (100 ng; solid bar). n=8-24, * $P<0.05$ for control (PBS) treatment compared with drug treatments. NS, no significant pair-wise differences between drug treatments.

Supplementary Figure S19

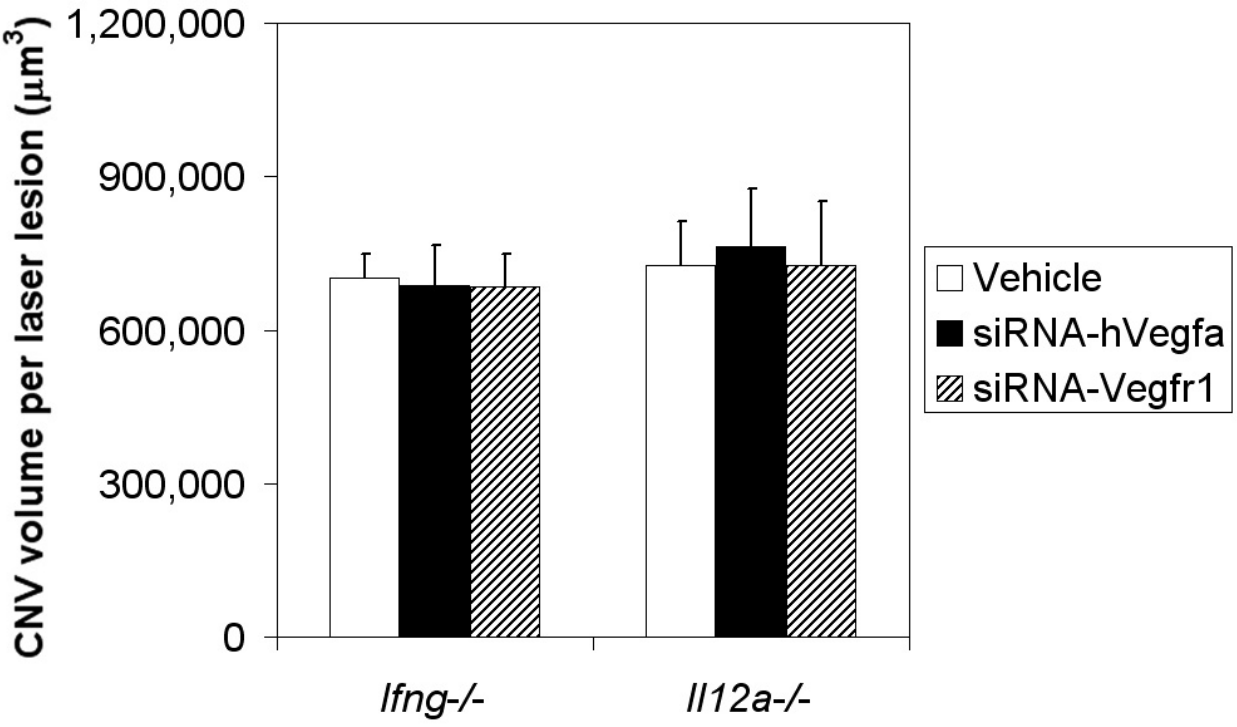

Targeted siRNA required IFN-γ and IL-12 to suppress CNV. Intravitreous administration of siRNA-h*Vegfa* or siRNA-*Vegfr1* (both 1 µg) did not suppress CNV in *Ifng*$^{-/-}$ or *Il12a*$^{-/-}$ mice. n=6. No significant differences compared to vehicle (siRNA buffer).

Supplementary Figure S20

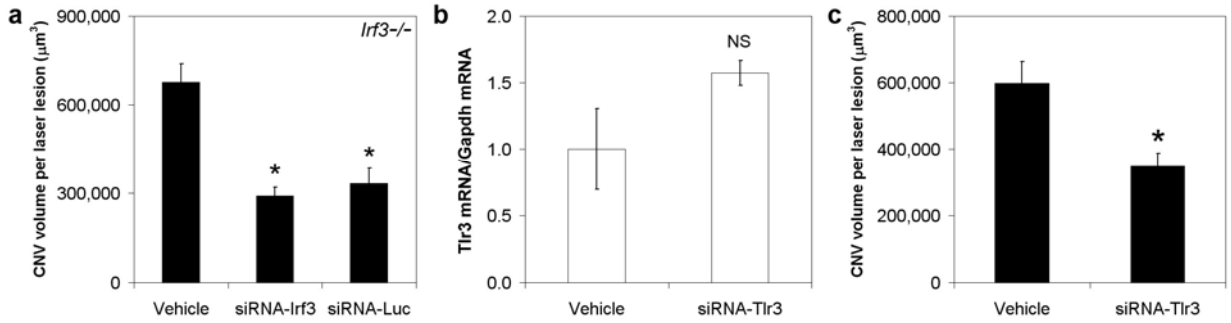

Targeted siRNA suppressed CNV not via target knockdown. a, Intravitreous administration of siRNA-*Irf3* suppressed CNV as effectively as siRNA-*Luc* (both 1 μg) in *Irf3*$^{-/-}$ mice. n=8-9. **b,c,** Intravitreous administration of siRNA-*Tlr3* (1 μg) in wild-type mice did not reduce *Tlr3* mRNA, as monitored by real time RT-PCR and normalized to *Gapdh* mRNA levels and to vehicle-treated levels (**b**) but did suppress CNV (**c**). n=4-6. (**a,c**) * $P < 0.05$ compared to vehicle (siRNA buffer). (**b**) NS, not significant (P=0.40).

Supplementary Figure S21

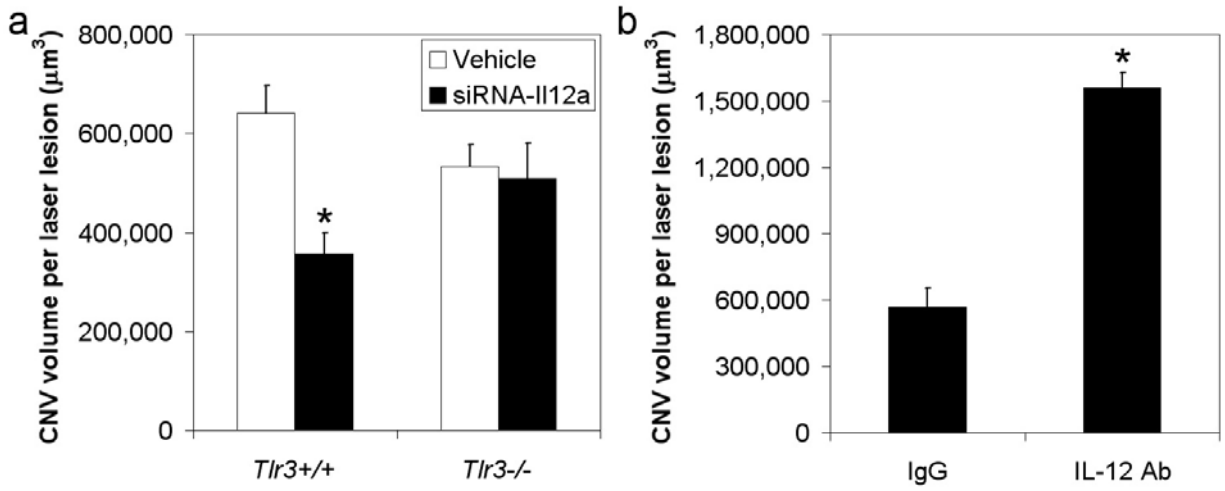

siRNA targeting anti-angiogenic gene suppressed CNV. a, Intravitreous administration of siRNA-*Il12a* (1 µg) suppressed CNV in *Tlr3*$^{+/+}$ but not *Tlr3*$^{-/-}$ mice. n=5-6, * $P < 0.05$ compared to vehicle (siRNA buffer). **b,** Intravitreous administration of neutralizing anti-IL-12 antibodies (Ab; 150 ng) increased CNV in wild-type mice. n=5-6, * $P < 0.05$ compared to isotype control IgG.

Supplementary Figure S22

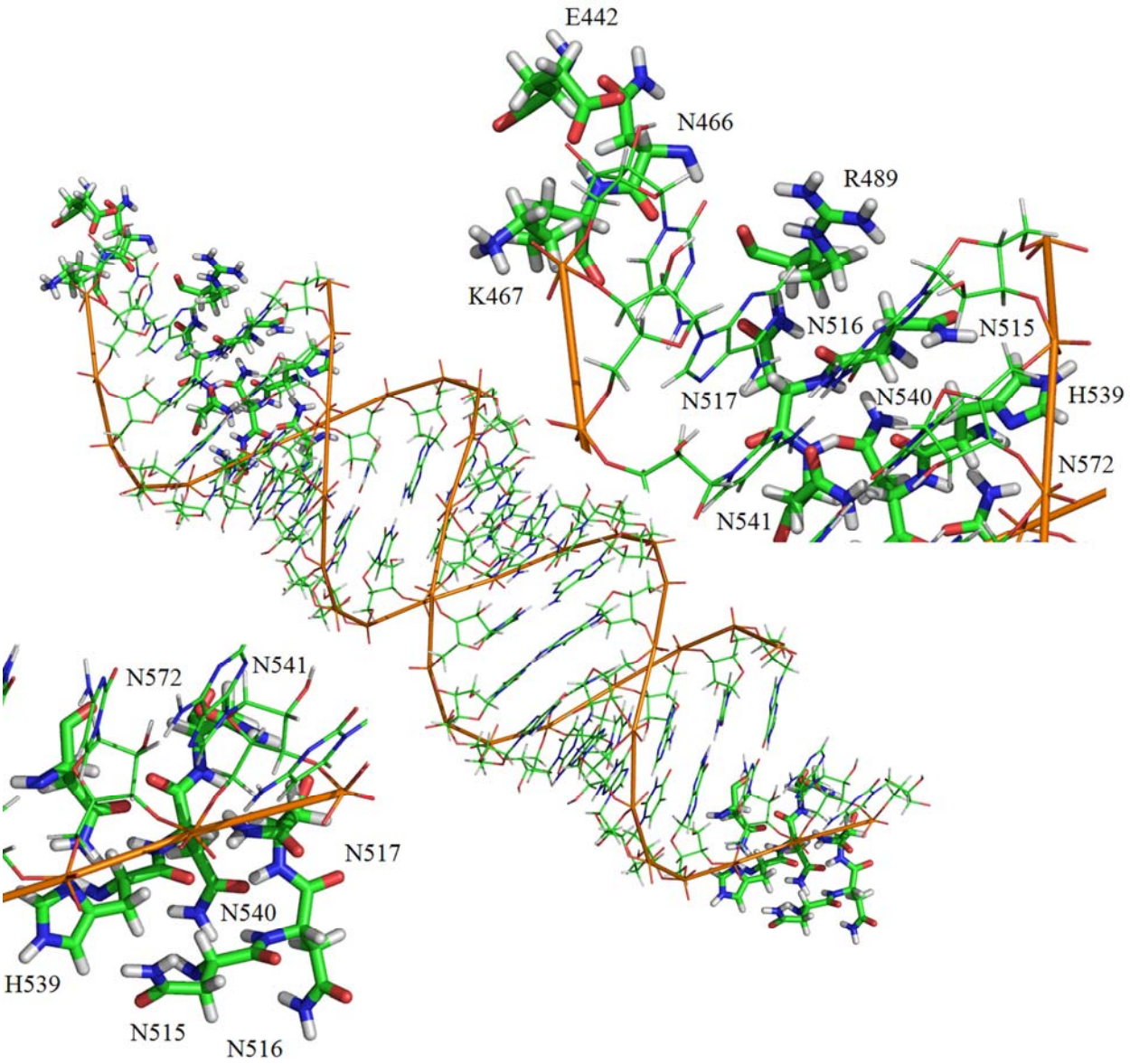

Docked 21-nt (19-nt duplex + 2-nt overhang) RNA shown along with TLR3 amino acid sidechains (labelled) of residues for which there is at least some evidence of involvement in RNA binding and/or TLR3 activation (residues shown all had intermolecular contacts with RNA of less than 4.5 Å). The docked 21-nt dsRNA could make contact with more distant residues (e.g. E442, N446 and K467) on at least one of the TLR3 monomers, for a total of 18 putative RNA-binding residue contacts for the entire complex.

Supplementary Figure S23

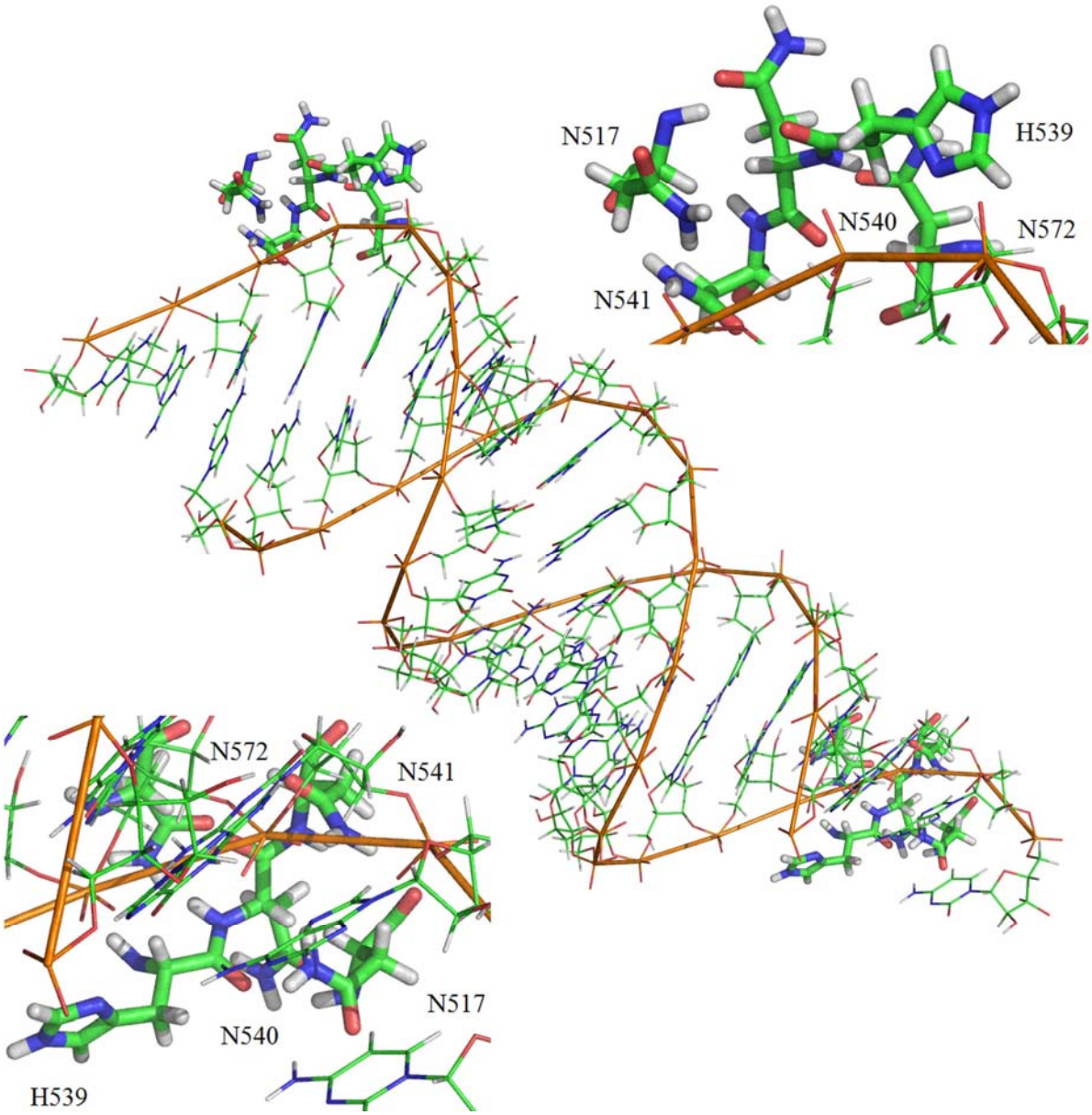

Docked 19-nt (17-nt duplex + 2-nt overhang) RNA shown along with putative RNA-binding TLR3 amino acid sidechains as described for Fig. S22. The shorter 19-nt dsRNA failed to make contact with as many of these residues as the 21-nt dsRNA, with only 10 putative RNA-binding residue contacts. Energy calculations on the optimized complexes suggested that binding of the 19-nt dsRNA to the TLR3 dimer was approximately 300 kcal/mol less favourable than that of the 21-nt dsRNA.

Supplementary Figure S24

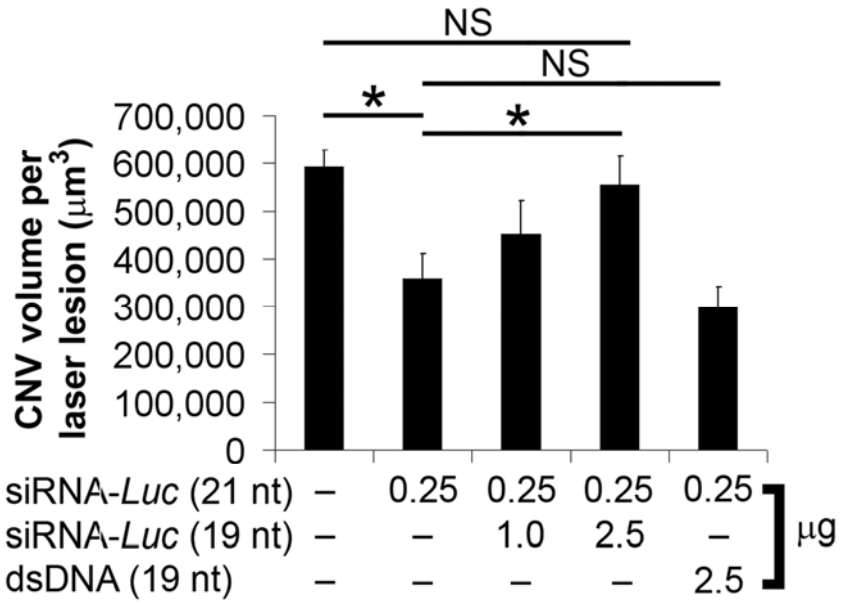

Short siRNA competitively antagonizes TLR3. 19-nt siRNA-*Luc* (1-2.5 μg), but not 19-nt dsDNA (2.5 μg), antagonized the ability of 21-nt siRNA-*Luc* (0.25 μg) to suppress CNV in wild-type mice. Reagents were injected intravitreously. n=7-11, * $P<0.05$, NS, not significant.

Supplementary Figure S25

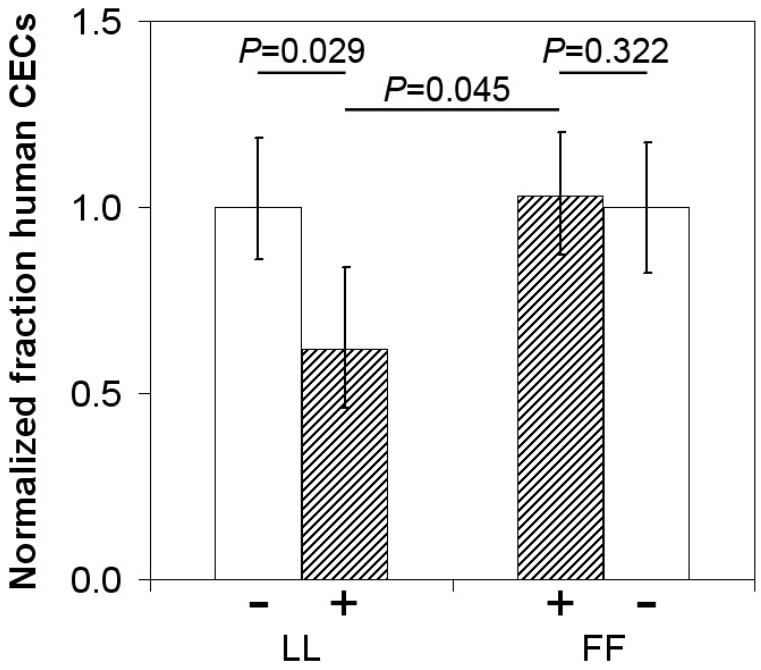

L412F SNP conferred resistance to siRNA-induced cytotoxicity. Exposure to serum-stable 2'O-methyl siRNA-*Luc* (20 µg/ml) for 48 h reduced viability of serum-supplemented cultures of primary human choroidal endothelial cells (hCECs) expressing the major allele LL at amino acid 412 of TLR3 but not of hCECs expressing the FF coding variant. The mean numbers of viable cells in the presence of siRNA (**+**) normalized to the number of viable cells in the absence of siRNA (**–**) plated are depicted with 95% c.i. ranges. n=6.

Supplementary Figure S26

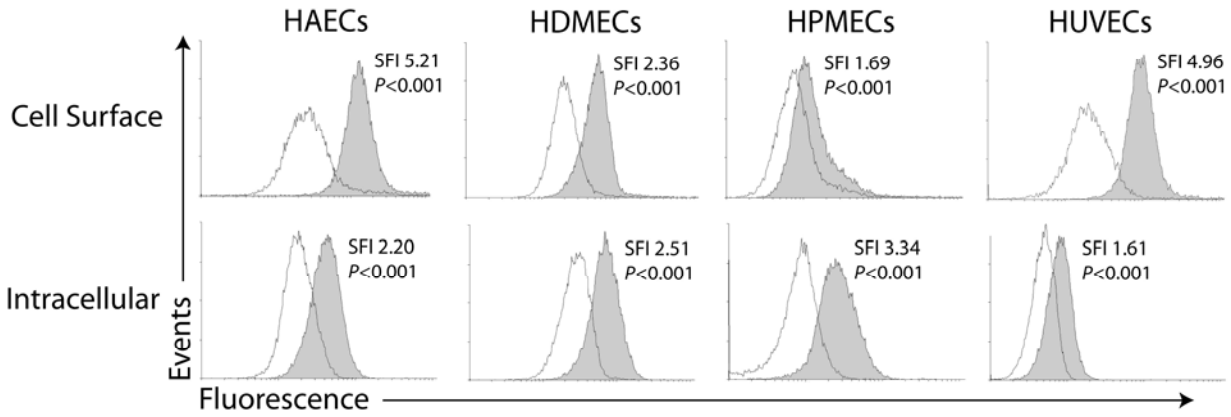

TLR3 expressed by various human endothelial cells. Flow cytometry detected the presence of TLR3 on the surface (top row) and in the intracellular space (bottom row) of human aortic endothelial cells (HAECs), human dermal microvascular endothelial cells (HDMECs), human pulmonary microvascular endothelial cells (HPMECs), and human umbilical vein endothelial cells (HUVECs). n=3-4. SFI, standardized fluorescence index (ratio of geometric means of cell populations), *P* values reflect statistical comparison between curves.

Supplementary Figure S27

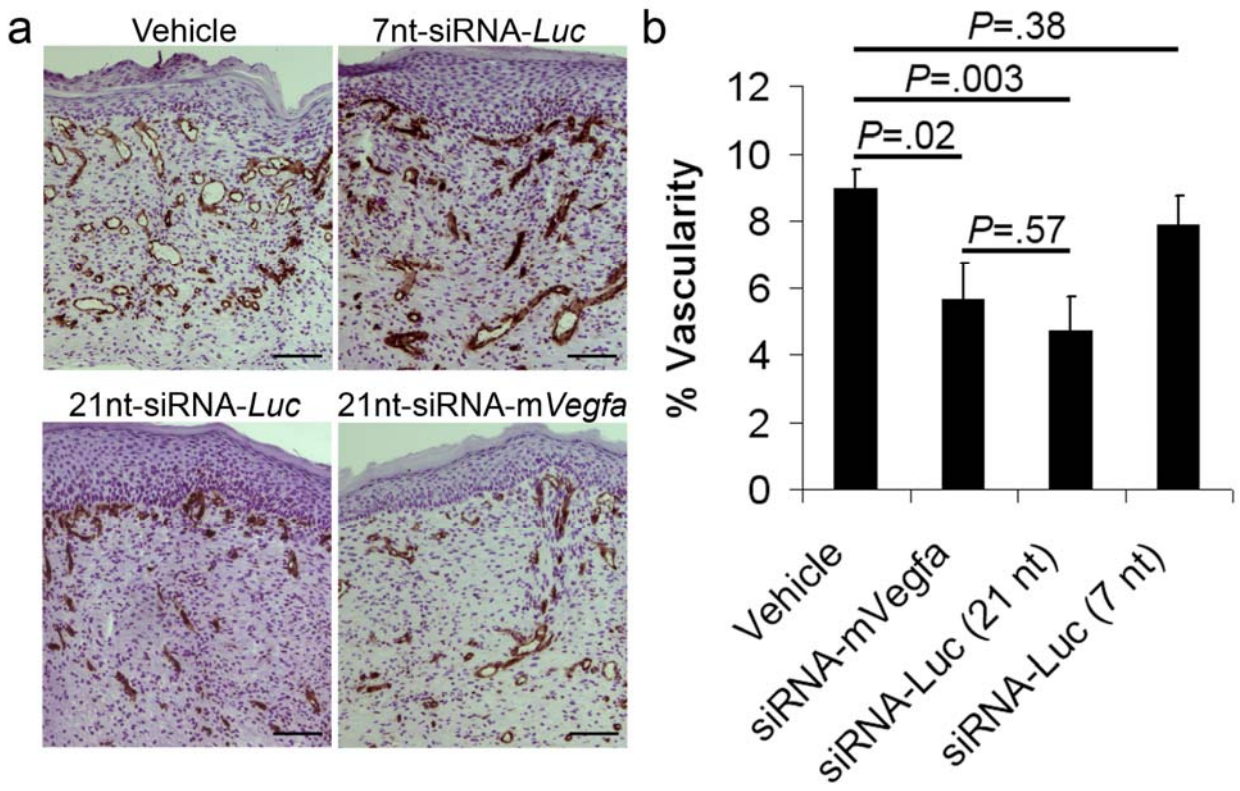

Non-targeted siRNA suppresses dermal neovascularization. a, Representative images of skin wounds in mice show that (**b**) topical application of serum-stable 2'*O*-methyl-modified 21-nt siRNA-*Luc* or 21-nt siRNA-m*Vegfa* (both 1 μg), but not 7-nt siRNA-*Luc* (0.3 μg), on days 0 and 2 after excisional dermal wounding in wild-type mice suppressed the area of dermis occupied by $CD31^+$ blood vessels (brown) (% vascularity) 7 days after injury. Slides counterstained with haematoxylin. Scale bar, 100 μm. n=4-6.

Supplementary Methods

Animals. C57Bl/6J, *Ifng*$^{-/-}$, *Il12a*$^{-/-}$, *Nfkb1*$^{-/-}$, *Tlr3*$^{-/-}$, *Tlr3*$^{+/+}$, and *Trif*^{Lps2} mice were purchased from The Jackson Laboratory. Balb/C mice were purchased from Taconic. *Vegfr1 tyrosine kinase*$^{-/-}$ (gift of M. Shibuya), *Ifnar1*$^{-/-}$ (gift of H.W. Virgin), *Irf3*$^{-/-}$ (gift of T. Taniguchi via M. David), *Prkra*$^{-/-}$ (gift of R.H. Silverman via G. Luo) and *Tlr7*$^{-/-}$ (obtained from S. Akira via D.A. Golenbock) mice have been previously described[1-4]. Mice were anesthetized by intraperitoneal injection of ketamine (50 mg/kg; Ft. Dodge Animal Health) and xylazine (10 mg/kg; Phoenix Scientific Inc.), and pupils were dilated with topical tropicamide (1%; Alcon Laboratories Inc.). Experiments were approved by institutional review boards and conformed to the Association for Research in Vision and Ophthalmology Statement on Animal Research.

CNV. Laser photocoagulation (532 nm, 200 mW, 100 ms, 75 μm) (OcuLight GL, IRIDEX Corporation) was performed on both eyes (4 spots per eye for volumetric analyses; 16 spots/eye for all other analyses) of each 6-8-week-old male mice to induce CNV as previously described [5,6]. CNV volumes were measured by scanning laser confocal microscope (TCS SP, Leica) as previously reported[5,6] with 0.5% FITC-conjugated *Griffonia simplicifolia* Isolectin B4 (Vector Laboratories) or 0.5% FITC-conjugated rat anti-mouse CD31 (BD Biosciences), or by cardiac perfusion with 5 mg/ml FITC-dextran (2 million average weight; Sigma-Aldrich). Pairwise correlations among volumes obtained by lectin, CD31, and dextran staining were highly correlated ($r^2 > 0.90$). CNV volumes per laser lesion were compared by hierarchical logistic regression using repeated measures analysis as previously described[5,6]. Results are expressed as mean ± s.e.m. Type-I error not exceeding 0.05 was deemed significant.

Drug treatments. siRNAs formulated in siRNA buffer (20 mM KCl, 0.2 mM MgCl2 in HEPES buffer at pH 7.5; Dharmacon) or phosphate buffered saline (PBS; Sigma-Aldrich), chloroquine (Invivogen), poly I:C (Invivogen), poly dI:dC (Invivogen), poly I:C12U (Ampligen; Bioclones); recombinant soluble (s) mouse TLR3 (R&D Systems), mouse sTLR4 (R&D Systems), neutralizing rat antibodies against mouse TLR3 (eBioscience; ref. [7]), immunostimulatory CpG oligonucleotide (ODN), GpC ODN (Invivogen), recombinant IFN-γ (Peprotech), recombinant IL-12 (eBioscience), neutralizing rat antibodies against mouse IL-12 (R&D Systems), isotype control IgGs (R&D Systems or eBioscience as appropriate) were dissolved in phosphate buffered saline (PBS; Sigma-Aldrich), and injected into the vitreous cavity in a total volume of 1 μl with a 33-gauge Exmire microsyringe (Ito Corporation). In some experiments, siRNA or vehicle was injected intraperitoneally.

siRNA. Chemical siRNA sequences and modifications are listed in the Supplementary Table. All siRNAs except RS3-RS6 (Ambion, Inc.) were purchased from Dharmacon. Sense and anti-sense strands of siRNA were annealed per the manufacturer's instructions and formulated in either sterile siRNA buffer (Dharmacon, Inc.) or nuclease-free PBS.

RNase digestion. siRNA-*Luc* was incubated with Benzonase® (>250U/μl) (Novagen) and $MgCl_2$ (2 mM) for 24 h at 37 °C. Benzonase was inactivated with 150 mM NaCl, and siRNA-*Luc* was recovered by ethanol precipitation. After several washes in 70% ethanol, the pellet was resuspended in sterile PBS.

DNV. Female Balb/c mice (8 weeks old) were used. Under isoflurane (Abbott Laboratories) anaesthesia, the dorsum of each mouse was shaved and wiped with 70% isopropyl alcohol. Six 3-mm full-thickness excisional wounds were made on each mouse as previously described[8]. Immediately following wounding and at 48 h post-wounding, each wound was treated topically

with 5 µl of sterile PBS or serum stable 2'O-methyl-siRNAs in PBS. Mice were sacrificed and wounds were harvested 7 d post-wounding. Samples were frozen in TBS tissue freezing media (Triangle Biomedical Sciences) for immunohistochemistry. Immunohistochemical staining for the endothelial cell marker CD31 was used to identify blood vessels in 5 µm cryosections from the middle portion of the wounds. Sections were thawed and fixed in acetone for 15 min. After three washes in PBS, pH 7.4, sections were treated with 0.3% H_2O_2 in methanol for 30 min to quench endogenous peroxidase activity. The slides were washed in PBS and blocked with normal rabbit serum (1:10, Sigma Chemical Company, St. Louis, MO) in PBS, for 30 min. Sections were incubated with 1.0 µg/ml of MEC13.3 rat anti-mouse PECAM-1 antibody (anti-CD31; BD Pharmingen, San Diego, CA) in 10% normal rabbit serum. After a 30 min incubation with PECAM-1 primary antibody, the slides were washed in PBS. Sections were then incubated for 30 min with 13.3 µg/ml of mouse adsorbed biotinylated rabbit anti-rat IgG antibody (Vector Laboratories, Burlingame, CA) in 10% normal rabbit serum. After washes in PBS, all slides were incubated with avidin-biotin-horseradish peroxidase complex, ABC-HRP (Vector Laboratories, Burlingame, CA) for 30 min, washed, then incubated with the HRP substrate 3,3'-diaminobenzidine (DAB; Kirkegaard and Perry Laboratories, Gaithersburg, MD) for 10 min. After counterstaining with Hematoxylin-2 (Richard Allen Scientific), the sections were dehydrated in alcohols, cleared in xylene (Richard Allen Scientific), and coverslips were applied with Cytoseal 280 (Stephens Scientific, Kalamazoo, MI). PECAM-stained wound sections were used to determine the density of blood vessels within wounds as outlined previously[8]. Briefly, images of stained sections were captured using Scion Image software (Scion Corporation, Frederick, MD). The total dermal area to be analyzed was outlined using a freehand drawing tool and measured, and the PECAM-positive area was also determined. Using these measurements,

the percentage of PECAM-positive vessels per total area analyzed (blood vessel density) was calculated.

Immunohistochemistry. Specificity was assessed by staining with control isotype non-immune IgG and by omitting the primary antibody.

Protein expression. Enzyme-linked immunosorbent assays (ELISAs) were used according to the manufacturer's instructions to quantify IFNs-α, β, γ (PBL Laboratories). Measurements were normalized to total protein (Bio-Rad).

Gene expression. Total mouse RPE/choroid RNA was prepared (RNAqueous, Ambion) and cDNA was synthesized by reverse transcription (Taqman, Applied Biosystems) and analyzed by real-time quantitative polymerase chain reaction (ABI 7000, Applied Biosystems). Primers used in PCR were: *Vegfa* (forward: 5'-GCCAGCACATAGGAGAGATGAGC-3'; reverse: 5'-CAAGGCTCACAGTGATTTTCTGG-3'); *Vegfr1* (forward: 5′-GAGGAGGATGAGGGTGTCTATAGGT-3′; reverse: 5′-GTGATCAGCTCCTGGTTTGACTT-3′); *Vegfr2* (forward: 5′-CCAGACAGACAGTGGGATGGTCCT-3′; reverse: 5′-TGGTCTGGTTGGAGCCTTCCGA-3′); *Gapdh* (forward: 5'-AACTTTGTGAAGCTCATTTCCTGGTAT-3';reverse: 5′-CCTTGC TGGGCTGGGTGGT-3′). Primers for TLR3 were purchased from Superarray. The PCR reaction was performed with the SYBRgreen mastermix (Applied Biosystems). In some experiments, *Vegfa* expression was quantified using the primers and probes described in ref. [9] and normalized to glyceraldehyde-3-phosphate dehydrogenase (*Gapdh*) levels by polymerase chain reaction with reverse transcription (RT–PCR) using Taqman gene expression assays (Applied Biosystems).

For analysis of *SIDT1*/*Sidt1* expression, total RNA (RNAqueuos, Ambion) was harvested from C57BL6/J mouse RPE/Choroid 1 day after laser photocoagulation and human CECs at 70-80% confluency. cDNA was generated using reverse transcriptase (Taqman, Applied Biosystems) and subjected to PCR (Multiplex, Eppendorf). The following primers and PCR amplification parameters were used: human *SIDT1* (forward: 5'-GCTCCGCAGCTCTGAAAAGGTCCTC-3'; reverse: 5'-GGATTCGGCCGGAGT TCCCTC-3'); human *GAPDH* (forward: 5'-AGCTCACTGGCATGGCCT TC-3'; reverse: 5'-CCTGTTGCTGTAGCCAAATTCG-3'); mouse *Sidt1* (forward: 5'-GACTCTGCACTCTGATGCGG-3'; reverse: 5'-AATGCTCAGCCACTAAGCGC-3'); mouse *Gapdh* (forward: 5'-AACTTTGTGAAGCTCATTTCCTGGTAT-3'; reverse: 5'-CCTTGCTGGGCTGGGTGGT-3'). PCR products were subjected to electrophoresis on a 1.5% agarose gel with ethidium bromide (0.5 μg/ml) and visualized by UV (UVP Bio-imager). Bands were determined to be specific based on expected amplicon size for each primer set.

Flow cytometry. *Surface and intracellular TLR3 on human ECs.* Human CECs, isolated as previously reported[10], HAECs (gift of E. Reed), HPECs (Clonetics), HDMECs (Clonetics), and HUVECs (Clonetics) were cultivated in MCDB-131 media (Gibco) supplemented with EGM-2MV (omitting gentamicin, hydrocortisone, Clonetics) at 37 °C and 5% CO_2. Cells (10^6) were harvested at 70-80% confluency with 0.04% EDTA followed by blocking in PBS-10% mouse serum containing 0.1 mg/ml of normal human IgG and 0.1% NaN_3. For surface TLR3 staining, cells were incubated with PE-conjugated anti-human TLR3 (20 μg/ml, Imgenex, Clone 40C1285.6) and an endothelial cell marker, FITC-conjugated CD31 (BD Biosciences, Clone WM59), for 30 min at 4 °C. For intracellular TLR3 staining, FITC-CD31 labelled cells were fixed and permeabilized with Leucoperm (Serotec) according to the manufacturer's instructions.

Cells were then stained with conjugated primary antibody for TLR3 (Imgenex) in the presence of 10% mouse serum for 30 min at RT. Surface and intracellular controls were stained with PE-conjugated mouse IgGκ1 isotype (BD Biosciences) at the same concentrations. Samples were resuspended in 1% PFA and analyzed on a FACSCalibur flow cytometer (Becton Dickinson) with Cellquest Pro (BD Biosciences) with a minimum of 10,000 events. Kolmogorov-Smirnov statistics were used to compare differences between groups.

Surface and intracellular TLR3 on mouse CECs. Suspensions of cells were isolated from mouse RPE/choroid 1 day after laser photocoagulation by incubation with collagenase D (20 U/l; Roche Diagnostics) and treated with Fc block (10 μg/ml; BD Biosciences) for 15 min on ice. Cells (10^6) were incubated with APC-conjugated anti-mouse CD31 antibody (20 μg/ml, BD Biosciences, Clone MEC13.3) and PE-conjugated anti-mouse VEGFR-2 antibody (20 μg/ml; BD Biosciences, Clone Avas12α1) to identify double positive endothelial cells. For surface TLR3 staining, cells were also incubated with a primary antibody for mouse TLR3 (10 μg/ml, R&D Systems, Clone MAB3005) that was pre-conjugated to Alexa Fluor 488 using a commercially available kit (Invitrogen) according to the manufacturer's instructions. For intracellular TLR3 staining, CD31/VEGFR2 labelled cells were subjected to fixation and permeabilization followed by incubation with the conjugated anti-TLR3 antibody (5μg/ml). FITC conjugated rat IgG2a isotype (BD Biosciences) was used at the same concentrations as a control for surface and intracellular samples. Cells were analyzed with a minimum of 10,000 events on a FACSCalibur flow cytometer.

Fluorescein-siRNA interaction assays. CD31/VEGFR-2 labelled RPE/choroid cells (10^6) isolated from wild-type C57BL/6J mice 1 day after laser photocoagulation were incubated with fluorescein- siRNA-*Luc* (100μg/ml) for 30 min at 4 °C in PBS-1% BSA. To determine the

specificity of siRNA binding to TLR3, fluorescein-siRNA-*Luc* was pre-incubated with either soluble TLR3 or TLR4 (R&D Systems) in greater than 1X molar excess for 30 min at 37 °C prior to incubating with RPE/choroid cells. To further demonstrate specificity of siRNA binding to surface TLR3, RPE/choroid cells were pre-incubated with poly I:C or poly dI:dC (1 mg/ml) for 30 min at 4 °C prior to staining with fluorescein-siRNA-*Luc*. Additionally, CD31/VEGFR-2 labelled RPE/choroid cells (10^6) isolated from *Tlr3*$^{-/-}$ mice 1 day after laser photocoagulation were evaluated for siRNA binding specificity. Samples were washed, fixed in 1% PFA, and analyzed on a FACSCalibur flow cytometer with a minimum of 10,000 events.

Fluorescein-siRNA uptake in mouse RPE/choroid cells. RPE/choroid cell suspensions were prepared from wild-type C57BL/6J mice immediately after laser photocoagulation. Cells (10^6) were incubated with 21-nt-fluorescein-siRNA-*Luc*, 21nt-fluorescein siRNA-*Luc*-chol (both 100 μg/ml) or PBS vehicle in phenol-free M199 media (Gibco) supplemented with 10% FBS for 1 h at 37 °C. Cells were washed in PBS and treated with 150 μl of 0.05% trypsin (Gibco) for 3 min at 37 °C to remove extracellular siRNA. Trypsin was then neutralized in M199 media with 10% FBS, and cells were washed in PBS-1% BSA three times. Samples were resuspended in 1% PFA and analyzed on a FACScalibur with a minimum of 10,000 events.

Immunofluorescent Microscopy. *Fluorescein-siRNA uptake in human CECs:* Primary human CECs (10^5) were harvested with 0.04% EDTA and incubated with 21-nt-fluorescein siRNA-*Luc* or 21nt-fluorescein siRNA-*Luc*-chol (both 100 μg/ml) for 1 h at 37 °C. Cells were washed with PBS, centrifuged onto slides (Shandon Cytospin 3) and imaged with confocal laser scanning microscopy (Leica SP-2).

Fluorescein-siRNA binding in mouse RPE/Choroid tissue: Frozen sections of wild-type or *Tlr3*$^{-/-}$ mice prepared 3 days after laser injury and intravitreous injection of siRNA-*Luc* (1 μg) were

blocked with 3% BSA for 1 h at 37 °C and incubated with 21-nt-fluorescein siRNA-*Luc* (10 μg/ml) for 1 h at 37 °C. Slides were then washed with PBS and fixed with 4% PFA for 10 min. For signal amplification, sections were then washed in PBS, blocked in 10% normal rabbit serum, and incubated with rabbit anti-FITC antibody (1:100, Zymed) overnight at 4 °C. Primary antibody was detected with anti-rabbit Alexa Fluor 488 (1:200, Molecular Probes) for 1 h at RT. Single (no primary) and double (no primary or secondary) controls were prepared in parallel. DAPI (Molecular Probes) was used as a nuclear counterstain. Sections were imaged by fluorescent microscopy (Nikon) with autofluorescence detection through the red channel.

TLR3 localization on mouse CECs: Mouse eyes were subjected to laser photocoagulation and intravitreous injection of siRNA-*Luc* (1 μg). Eyes were harvested on day 1, embedded in OCT and snap-frozen in liquid nitrogen. Sections (10 μm) were fixed in ice-cold acetone for 10 min at 4 °C, washed in PBS, and blocked with PBS-10% normal goat serum for 1 h at RT. Slides were incubated with rabbit anti-mouse TLR3 (1:50, Imgenex) overnight at 4 °C followed by washes and detection with goat anti-rabbit IgG conjugated to Alexa Fluor 594 (1:200, Molecular Probes). For labelling of endothelial cells, sections were incubated with rat anti-mouse CD31 (1:50, BD Biosciences, Clone MEC13.3) for 1 h at RT followed by detection with goat anti-rat IgG conjugated to Alexa Fluor 488 (1:200, Molecular Probes). Slides were treated with DAPI for nuclear counterstain and cover-slipped in Vectashield (Vector Labs).

TLR3 localization on human CECs: Human CECs were grown to 70-80% confluency in chamber slides (Lab-Tek). For surface staining, cells were blocked with PBS-1% BSA and incubated with mouse anti-human TLR3 (20 μg/ml, eBioscience, Clone TLR3.7) at RT for 1 h. For surface membrane colocalization, cells were stained with rabbit anti-CD46 (1:50, Santa Cruz). For secondary detection, cells were washed and then incubated with goat anti-mouse Alexa Fluor

488 (1:400, Molecular Probes) or donkey anti-rabbit Cy3 (1:400, Jackson Immunoresearch) for 1 h at RT. Following three washes in PBS, surface TLR3 stained cells were fixed in 0.05% PFA for 10 min. Mouse IgGκ1 isotype antibody (20 μg/ml, eBioscience) was used as a control. After DAPI counterstain, slides were cover-slipped in Vectashield (Vector Labs) and visualized with confocal laser scanning microscopy (Leica SP-5).

Single Nucleotide Polymorphism (SNP) Genotyping. Genomic DNA was extracted from human choroidal endothelial cells. For the rs3775291 SNP, oligonucleotide primers 5'-TCATTAAGGCCCAGGTCAAG-3' and 5'-TGGCTAAAATGTTTGGAGCA-3' were used for PCR amplification. For the rs5743316 SNP, the genomic DNA was amplified using PCR and the oligonucleotide primers 5'-TCCACCACCAGCAATACAAC-3' and 5'-TAGTTGTGGAAGCCAAGCAA-3'. The amplification parameters for the SNPs were 95 ˚C denature 5 min, 95 ˚C 30 s, 55 ˚C 30 s, 72 ˚C 1 min for 35 cycles, and 72˚ C extension for an additional 10 min. These SNPs were genotyped using the SNPSHOT method on an ABI 3130xl genetic analyzer (Applied Biosystems, Foster City, CA) according to the manufacturer's instructions. The oligonucleotide primers for the single base extension were 5'-GCTCATTCTCCCTTACACATA-3' for rs3775291 and 5'-ATGCTCGATCTTTCCTAC-3' for rs5743316.

Cell culture. Human CECs were isolated using mouse monoclonal anti-human CD31 antibody (BD Pharmingen) coated magnetic beads (Dynabeads; Dynal, Invitrogen) from anonymously donated human eyes obtained from the Oregon Lions Eye Bank, as previously described[10]. Genomic DNA was extracted using the QIAamp DNA Mini Kit (Qiagen). CECs were thawed and cultured in MCDB-131 medium (Sigma-Aldrich) with 2% foetal bovine serum (FBS; Hyclone) and endothelial growth factors (EG2 SingleQuot omitting gentamicin, hydrocortisone

and FBS; Clonetics, Cambrex Bioscience) at 37 °C and 5% CO_2, prior to seeding into 96-well plates in 0.1 ml of medium. After an overnight rest, CECs were stimulated for 24 h with the same volume of MCDB-131 medium, containing 2% FBS, and 1,000 U/ml IFNs-α,β (PBL Interferon Source). Subsequently the cells were incubated with 0.1 ml of MCDB-131 medium containing 2% FBS, endothelial growth factors, and, for test wells, 2O'-Me-siRNA-*Luc* (20 μg/ml). After 48 h, cell proliferation was measured using the CyQuant NF Cell Proliferation Assay Kit (Molecular Probes, Invitrogen). Fluorescence intensity was measured on a microplate reader (VICTOR^3 Multilabel Counter Model 1420, PerkinElmer Life) at RT within 2 h of equilibration of dye-DNA binding, with excitation set at 485 nm and emission detected at 530 nm. All conditions were assayed in quadruplicate. Linear mixed models were fitted into data by treating the factors as fixed (genotype, siRNA treatment, interaction between genotype and drug) or random (patients, replicates, interaction between siRNA and patients, measurement error) effects. An F test with numerator mean square for group by drug interaction and denominator interaction between siRNA and cells nested within genotype groups was conducted for the group by siRNA interaction. Log normalized means and 95% c.i. are presented.

Modelling. Rigid-body protein docking based on surface shape complementarity, using a grid-based molecular representation of the protein and RNA was employed, first to dock one TLR3 ectodomain (ECD) on another to form a symmetric dimer, and then to dock 21-nt and shorter dsRNAs separately to the ligand binding domains of the TLR3 dimer. As initial structures for the docking, we used the crystal structures of the TLR3 ligand binding domain (2A0Z) and a 19-bp RNA duplex (1QC0), modified by addition or deletion of bases to generate 21-nt (19 +2) or 19-nt (17 +2) dsRNA with 2 base overhangs set in A-form conformations. A Fast-Fourier Transform

(FFT) technique makes it possible to perform an exhaustive search and evaluation of the huge conformational space available in docking macromolecular complexes, particularly with the use of additional constraints based on available biological information, which greatly improves the performance of the docking procedure. A parallelized version of the rigid-body docking program, FTDock in the 3D-Dock suite[11], which was modified to accommodate biological constraints at the space sampling stage, was used to perform protein-protein and RNA-protein docking experiments to obtain TLR3-dsRNA complex models which are consistent with the experimental binding data available for their binding interface, as described in the main text. In the docking experiment, each grid distance was set to 0.8 Å and the Euler angle sets were generated using the same formula used in FTDock with a sampling interval of 9°. The top 3 scores after filtering at each orientation were collected and all scores were re-ranked. The docking modes were further analyzed using Residue Level Pair Potential Scoring (RPScore)[12] method which adjusts scores to accommodate statistics of known residue-residue interactions. Two TLR3 ECDs were first docked together, using weak amino acid pair constraints between the 2 monomers (within 20 Å distance) designed to give a C-terminus dimer in which the established RNA-binding patches of each monomer, involving N541, H539 and nearby residues, would be approximately 50 Å apart. This constraint was derived based upon the current data showing that dsRNA shorter than 21-nt failed to activated TLR3 signalling. The best docked model from this simulation was a highly symmetrical dimer with a H539 to H-539 alpha carbon separation of about 55 Å, and with the RNA-binding residues of each monomer on the same slightly concave surface of the dimer. This TLR3 dimer was then used as the starting structure and the two distinct dsRNAs (19-nt and 21-nt) were separately docked onto the protein dimer, using

interaction with N541 and H539 at < 5 Å distance as the only constraints. Results were further filtered by selection of the most symmetrical docking of the RNA with respect to the protein dimer. The docked structures were then minimized to refine the structure and a short molecular dynamics simulation was carried out with an implicit Generalized Born solvation model[13], to obtain MD trajectories. These trajectories were used to calculate the free energies of binding in each case using the MMPBSA module in AMBER9 (ref. [14]). For each complex, five time points were selected for energy minimization and free energy calculation, and the energy difference was compared using Mann-Whitney U test and confidence intervals generated for the difference between the means.

Supplementary Notes

1. Hiratsuka, S., Minowa, O., Kuno, J., Noda, T. & Shibuya, M. Flt-1 lacking the tyrosine kinase domain is sufficient for normal development and angiogenesis in mice. *Proc Natl Acad Sci U S A*. **95**, 9349-9354 (1998)
2. Muller, U. *et al.* Functional role of type I and type II interferons in antiviral defense. *Science*. **264**, 1918-1921 (1994)
3. Sato, M. *et al.* Distinct and essential roles of transcription factors IRF-3 and IRF-7 in response to viruses for IFN-alpha/beta gene induction. *Immunity*. **13**, 539-548 (2000)
4. Hemmi, H. *et al.* Small anti-viral compounds activate immune cells via the TLR7 MyD88-dependent signaling pathway. *Nat Immunol*. **3**, 196-200 (2002)
5. Nozaki, M. *et al.* Drusen complement components C3a and C5a promote choroidal neovascularization. *Proc Natl Acad Sci U S A*. **103**, 2328-2333 (2006)

6. Nozaki, M. *et al.* Loss of SPARC-mediated VEGFR-1 suppression after injury reveals a novel antiangiogenic activity of VEGF-A. *J Clin Invest*. **116**, 422-429 (2006)

7. Lin, Y., Liang, Z., Chen, Y. & Zeng, Y. TLR3-Involved Modulation of Pregnancy Tolerance in Double-Stranded RNA-Stimulated NOD/SCID Mice. *J Immunol*. **176**, 4147-4154 (2006)

8. Swift, M. E., Kleinman, H. K. & DiPietro, L. A. Impaired wound repair and delayed angiogenesis in aged mice. *Lab Invest*. **79**, 1479-1487 (1999)

9. Zhang, L. *et al.* Different effects of glucose starvation on expression and stability of VEGF mRNA isoforms in murine ovarian cancer cells. *Biochem Biophys Res Commun*. **292**, 860-868 (2002)

10. Smith, J. R. *et al.* Unique gene expression profiles of donor-matched human retinal and choroidal vascular endothelial cells. *Invest Ophthalmol Vis Sci*. **48**, 2676-2684 (2007)

11. Gabb, H. A., Jackson, R. M. & Sternberg, M. J. Modelling protein docking using shape complementarity, electrostatics and biochemical information. *J Mol Biol*. **272**, 106-120 (1997)

12. Moont, G., Gabb, H. A. & Sternberg, M. J. Use of pair potentials across protein interfaces in screening predicted docked complexes. *Proteins*. **35**, 364-373 (1999)

13. Tsui, V. and Case, D. A. Theory and applications of the generalized Born solvation model in macromolecular simulations. *Biopolymers*. **56**, 275-291 (2000)

14. Case, D. *et al.*, AMBER 9 (University of California, San Francisco, 2006).